Applied Surface Science 256 (2010) 2184–2188

Contents lists available at ScienceDirect

Applied Surface Science

journal homepage: www.elsevier.com/locate/apsusc

# Field emission characteristics of carbon nanotubes post-treated with high-density Ar plasma

Wen-Pin Wang [a], Hua-Chiang Wen [b], Sheng-Rui Jian [c,*], Huy-Zu Cheng [c], Jason Shian-Ching Jang [d], Jenh-Yih Juang [e], Huang-Chung Cheng [f], Chang-Pin Chou [a]

[a] Department of Mechanical Engineering, National Chiao Tung University, Hsinchu 300, Taiwan
[b] Department of Mechanical Engineering, Chin-Yi University of Technology, Taichung 400, Taiwan
[c] Department of Materials Science and Engineering, I-Shou University, No. 1, Sec. 1, Syuecheng Rd., Kaohsiung 840, Taiwan
[d] Department of Mechanical Engineering & Institute of Materials Science & Engineering, National Central University, Chung-Li 320, Taiwan
[e] Department of Electrophysics, National Chiao Tung University, Hsinchu 300, Taiwan
[f] Department of Electronic Engineering, National Chiao Tung University, Hsinchu 300, Taiwan

ARTICLE INFO

*Article history:*
Received 22 May 2009
Received in revised form 18 September 2009
Accepted 18 September 2009
Available online 26 September 2009

*Keywords:*
Multi-walled carbon nanotube
Scanning electron microscopy
Field emission property
Transmission electron microscopy

ABSTRACT

The field emission characteristics of carbon nanotubes (CNTs) grown by thermal chemical vapor deposition (CVD) and subsequently surface treated by high-density Ar plasma in an inductively coupled plasma reactive ion etching (ICP-RIE) with the various plasma powers were measured. Results indicate that, after treated by Ar plasma with power between 250 and 500 W, the emission current density of the CNTs is enhanced by nearly two orders of magnitude (increased from 0.65 to 48 mA/cm$^2$) as compared to that of the as-grown ones. Scanning electron microscopy (SEM) and transmission electron microscopy (TEM) were employed to investigate the structural features relevant to the modified field emission properties of CNTs. The SEM images of CNTs subjected to a 500 W Ar plasma treatment exhibit obvious damages to the CNTs. Nevertheless, the turn-on fields decreased from 3.6 to 2.2 V/μm, indicating a remarkable field emission enhancement. Our results further suggest that the primary effect of Ar plasma treatment might be to modify the geometrical structures of the local emission region in CNTs. In any case, the Ar plasma treatment appears to be an efficient method to enhance the site density for electron emission and, hence markedly improving the electric characteristics of the CNTs.



## 1. Introduction

Since its first discovery by Iijima in 1991 [1], carbon nanotubes (CNTs) have attracted tremendous scientific and technological interest because of their exceptional structural, electrical and mechanical characteristics [2] for many potential applications, including that the high-strength composites [3], energy storage [4], nanofabrication [5], etc. In particular, the field emission has been considered as one of the most promising characteristics of CNTs to be realized for immediate applications owing to the favorable features for field emitters, such as high aspect ratio, high electrical conductivity, high mechanical strength, high chemical stability, as well as high thermal conductivity inherent to CNTs [6–8].

Indeed, excellent field emission properties, namely high emission current density, low emission threshold voltage, and long lifetime have been demonstrated for emitters made of CNTs [7]. Nevertheless, in order to optimizing the field emission properties for large area applications, it is highly desirable to produce vertically aligned CNTs with optimal combinations of density, diameter and length on the substrates. The field emission properties of CNTs are often affected by these factors, especially in the device applications [9,10]. Consequently, synthesizing CNTs on catalytic transition metal patterned substrates by chemical vapor deposition (CVD) systems have been widely used for obtaining better control of those parameters [8]. Unfortunately, contamination has been known to occur on the surface of CNTs, which may affect the stability of the emission process and reduces their efficiency. In order to enhance the field emission properties of CNTs, some effective methods are required to investigate the fundamental issues involved in optimizing the performance of CNTs. For instance, plasma surface treatment on the surface of carbon-based materials has been proposed to reduce the contamination [11–13] and has shown significant improvements in field emission characteristics [13]. However, there is still plenty of room for further improvements. In particular, to our knowledge, little work has been systematically carried out on how purifying

* Corresponding author. Tel.: +886 7 6577711x3130; fax: +886 7 6578444.
*E-mail address:* srjian@gmail.com (S.-R. Jian).

0169-4332/$ – see front matter © 2009 Elsevier B.V. All rights reserved.
doi:10.1016/j.apsusc.2009.09.070

the amorphous phase carbon and removing the catalytic nanoparticles on the surface of CNTs will affect the emission characteristics of CNTs.

The aim of the present study is to investigate the field emission characteristics of CNTs grown by thermal CVD method. The CNTs were further post-treated by high-density Ar plasma in an inductively coupled plasma reactive ion etching (ICP-RIE). The maximum emission current density obtained for CNTs post-treated by Ar plasma was 48 mA/cm$^2$. It translates into about two orders of magnitude enhancement over that of the as-grown CNTs. In addition, the field enhancement factor ($\beta$) obtained from the Fowler–Nordheim (FN) tunneling model is estimated to be ~3500 for the Ar plasma post-treated CNTs as compared to ~1900 for the as-grown samples. It is indicative that some geometric shape modifications on CNTs might be also involved in plasma treatments.

## 2. Experimental details

Experimentally, CNTs were synthesized selectively on patterned p-type Si(1 0 0) substrates utilizing a thermal chemical vapor deposition (CVD) system with a mixture of $CH_4/C_2H_4/N_2/H_2$ gases. The gas flow rate was maintained at 200/10/500/500 sccm (standard cubic centimeter per minute at standard temperature and pressure, STP). The substrate temperature during growth was estimated to be 700 °C and the growth time was 10 min.

The schematics of the CNT growth processes conducted in the current study are illustrated in Fig. 1(a). Firstly, conventional semiconductor lithography technique was employed to pattern the Si substrate. Subsequently, a layer of 50 nm-thick titanium (Ti) film was deposited onto the substrate by electron beam evaporation. Then, without breaking the vacuum, a 5 nm-thick Fe–Ni catalytic layer was deposited onto the Ti film. Here, the Ti layer acts as a diffusion barrier layer for the catalyst to prevent from forming nickel silicide during CNT growth at high temperatures. In this way, although titanium silicide may still form during CNT growth, the catalytic activities of the Fe–Ni catalyst remain active for CNTs growth. Remnant catalyst and Ti layers on the photoresist were removed by an acetone lift-off technique. Finally, CNTs were formed selectively on the catalyst-patterned Si substrates. To investigate the effects of post-deposition treatments on the emission characteristics of CNTs, series of samples were post-treated in an inductively coupled plasma reactive ion etching (ICP-RIE) system with various ICP powers of 250, 300, 400 and 500 W, respectively. The pressure in ICP-RIE system was 10 mTorr and the Ar flow rate was 20 sccm. Fig. 1(b) displays the schematics of the diode device type setup used in characterizing the field emission properties of CNTs. The device was operated in high-vacuum environment with a base pressure of $1 \times 10^{-4}$ mTorr. An indium tin oxide (ITO) glass coated with a layer of phosphor was employed as the anode. The spacing between the anode and CNTs surface was kept at about 100 μm. The emission current densities of CNTs were measured using a Keithley 237 high voltage source measure units and an IEEE 488 interface was controlled by a personal computer.

The morphology and structure of the CNTs samples were analyzed by the field emission scanning electron microscopy (FESEM: Hitachi S-4700, Tokyo, Japan). The structural changes in CNTs caused by the surface treatments were investigated by a Raman microspectroscopy equipped with an argon ion laser operating at a wavelength of 514.5 nm with a charge coupled device detector. The samples were imaged with a 100× objective lens under the microscope and laser beam with a power of 50 mW was directed onto the selected spots at the sample. High-resolution transmission electron microscopy (HRTEM: JEOL JEM-3011, Tokyo, Japan) was also used to characterize the microstructures of CNTs.

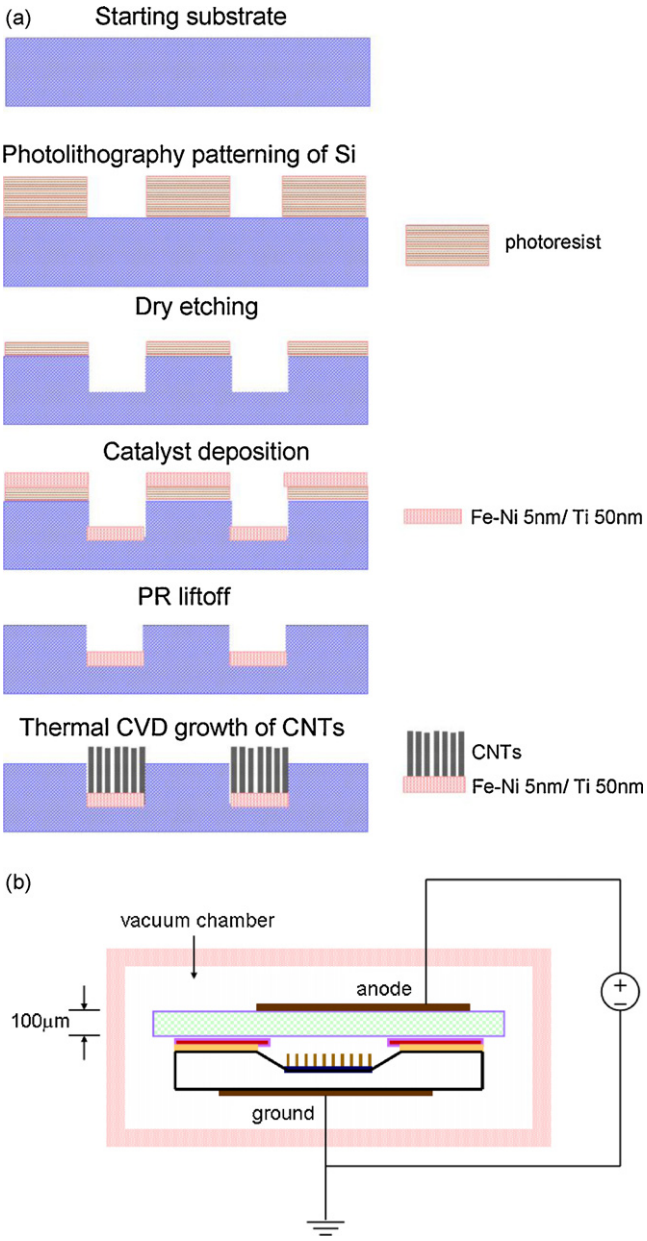


**Fig. 1.** (a) Schematic diagrams of the growth processes of CNTs and (b) field emission current measurement system.

## 3. Results and discussion

The correlation between Ar plasma treatments and field emission properties of CNTs is investigated by analyzing the results obtained from several independent techniques such as FESEM, TEM and Raman spectroscopy techniques. Fig. 2 shows the FESEM micrographs of a gated CNTs microcathode under the conditions of untreated pristine CNTs (Fig. 2(a)) and that subjected to the Ar plasma treatments at ICP power of 300 W (Fig. 2(b)) and 500 W (Fig. 2(c)), respectively. Apparent differences between the pristine and plasma-treated CNTs are immediately evident. For instance, unlike that exhibited in Fig. 2(a), the impurities on the surface of CNTs are absent in samples treated at an ICP power of 300 W (Fig. 2(b)). Moreover, the morphology of the CNTs in the latter case appears to be more vertically aligned and bundled. However, as shown in Fig. 2(c) for samples treated at an ICP power of 500 W, excessive ICP power apparently has led to serious damages in the CNTs.

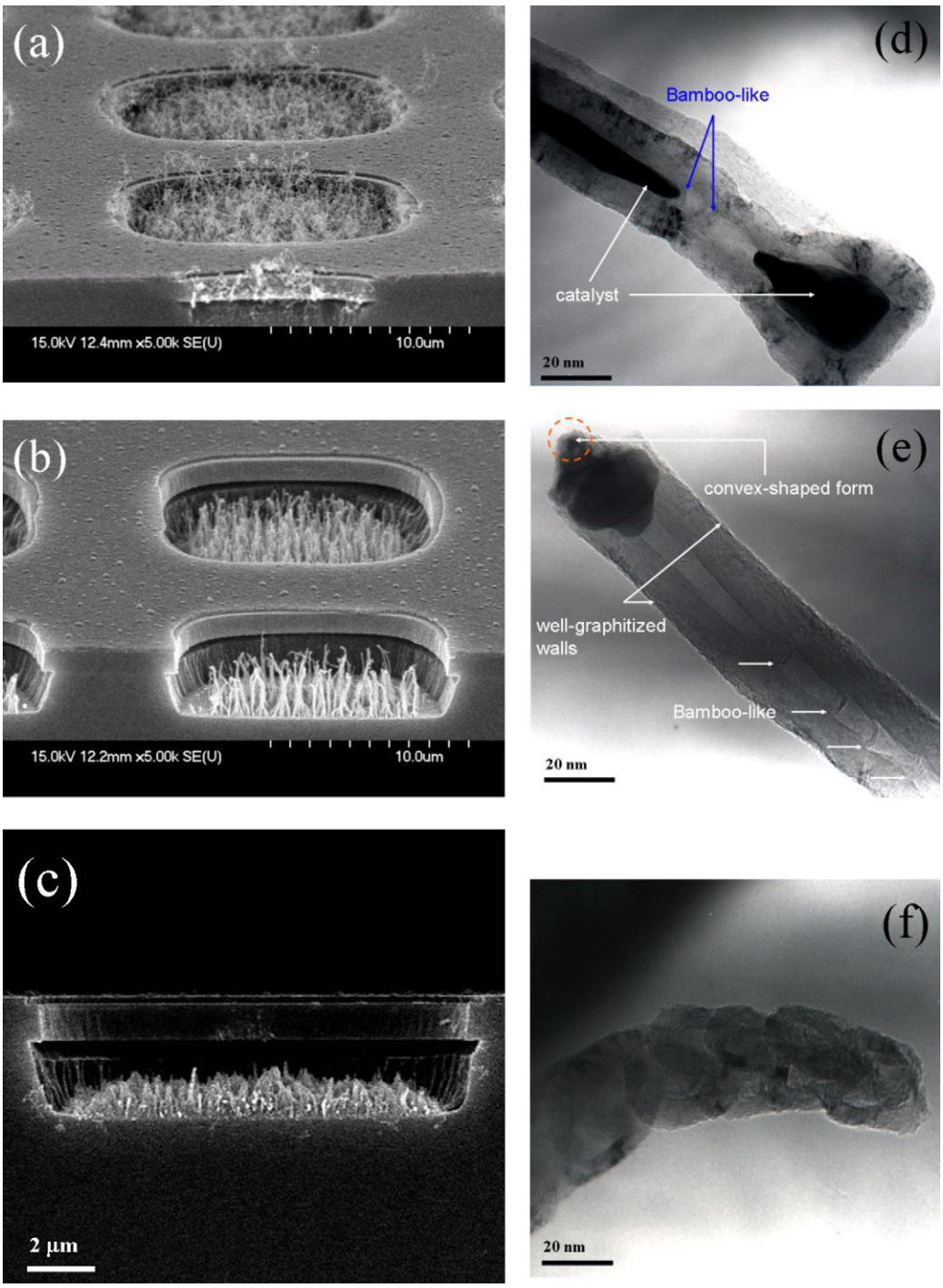


**Fig. 2.** SEM images of CNTs samples (a) untreated and, (b) and (c) subjected to Ar plasma post-treatment of 300 and 500 W, respectively; corresponding to TEM micrographs of (d)–(f) are displayed.

In order to further compare the possible structural changes introduced by Ar plasma treatment, TEM analyses were performed. The typical results for the CNTs respectively shown in Fig. 2(a)–(c) are displayed in Fig. 2(d)–(f). For the as-grown CNTs (Fig. 2(d)), the catalytic nanoparticle was evidently observed to present at the tip of CNTs, suggesting that the current deposition conditions and the catalyst chosen favored the tip-growth diffusion mechanism [14]. The TEM image displayed in Fig. 2(e), on the other hand, reveals the typical structure of CNTs after being treated by Ar plasma with an ICP power of 300 W. In addition to the surface morphology changes described previously in SEM observation, the TEM image exhibits that the well-graphitized wall segments not only outgrew densely but also became more straightened along the nanotube walls (Fig. 2(e)). Furthermore, as can be seen in Fig. 2(a) and (b), not only the bamboo-like structure within the tube has been significantly modified by plasma treatments but also the tip of the tube was sharpened, as well. Since the bamboo-like structure has been identified to be highly defective and might be responsible for the enhanced emission performance in previous studies [15,16], we believe that the current observations on the microstructure modification may also lead to similar consequences to be explained later on.

**Table 1**
List of current density, turn-on field, field enhancement factor and Raman ratio ($I_D/I_G$) of CNTs before and after Ar plasma treatment.

| Conditions | Current density, $J$ (mA/cm$^2$) (@ $E$ = 5 V/μm) | Turn-on field, $E$ (V/μm) (@ $J$ = 10 μA/cm$^2$) | Field enhancement factor ($\beta$) | $I_D/I_G$ |
|---|---|---|---|---|
| As-grown | 2.35 | 3.1 | 1869 | 0.75 |
| 250 W | 12 | 2.7 | 3008 | 0.69 |
| 300 W | 48 | 2.2 | 3463 | 0.68 |
| 400 W | 3.18 | 3.2 | 1956 | 0.78 |
| 500 W | 0.65 | 3.6 | 1631 | 0.79 |

In addition to the direct morphological and microstructure analyses, Raman spectroscopy serves as an alternative unique tool for characterizing the average population of various types of CNTs consisting of the CNT film in a nondestructive manner [17]. The Raman spectra (not shown here) of CNTs grown with catalytic nanoparticles display two distinctive peaks, D (~1360 cm$^{-1}$) and G (~1580 cm$^{-1}$) modes, corresponding to the disorder-induced D-band and the stretching mode in the graphite plane or order carbon [18], respectively. The intensity ratio ($I_D/I_G$) has been further indicated to directly relate to the size of the sp$^2$ carbon cluster in the graphene sheet and, is nearly proportional to the defect density [19]. The $I_D/I_G$ ratio for all CNTs samples are obtained and listed in Table 1. It is evident that, after treated with Ar plasma operated at a power of 300 W, more ordered CNT constituent is present, which in turn results in a decreasing $I_D/I_G$ value obtained from the Raman signal. This is, in fact, consistent with the microstructure observations described above, where not only CNT tip structure was trimmed sharper but also removals of some disordered top layers were observed (as shown in Fig. 2(e)). Although high quality and defect-free CNTs are critical for fundamental studies and, sometimes, specific device applications, it is not necessary true for vacuum devices, such as field emitters discussed here. Indeed, HRTEM analysis on the microstructure of CNTs grown on carbon cloth suggested that CNTs with poorer crystallinity and more amorphous phases have exhibited better performance for field emitter applications [20]. It is generally conceived that defects may have played an important role in promoting the field enhancement factor during the field emission process, as suggested by the general occurrence of lower turn-on field for field emitters made of these "defective" CNTs. In order to further examine the validity of the abovementioned assessments, the emission current density and turn-on field of the Ar plasma-treated CNTs are discussed in detail in the following.

Fig. 3(a) displays a plot of the emission current density as a function of the electric field for CNTs obtained under various conditions. It is evident, again, that the CNTs properly treated by the Ar plasma exhibit much superior field emission properties with much lower threshold field and higher emission current density. In addition, the Fowler–Nordheim (FN) plots displayed in Fig. 3(b) also show that the FN characteristics are significantly enhanced via Ar plasma treatment. The emission current density, $J$ (A/cm$^2$), can be expressed as the following FN equation [21,22]:

$$J = \frac{I}{A} = \frac{k_1 \beta^2 E^2}{\phi} \exp\left(-k_2 \frac{\phi^{3/2}}{\beta E}\right) \quad (1)$$

where $k_1 = 1.54 \times 10^{-6}$ A eV V$^{-2}$, $k_2 = 1.54 \times 10^{-6}$ eV$^{-3/2}$ V cm$^{-1}$, $I$ is the emission current, $A$ is the emission area, $\beta$ is the enhancement factor, $E$ is the applied electric field, and $\phi$ is the work function. The equation can be further expressed as:

$$\frac{J}{E^2} = \frac{k_1 \beta^2}{\phi} \exp\left(-k_2 \frac{\phi^{3/2}}{\beta E}\right) \quad (2)$$

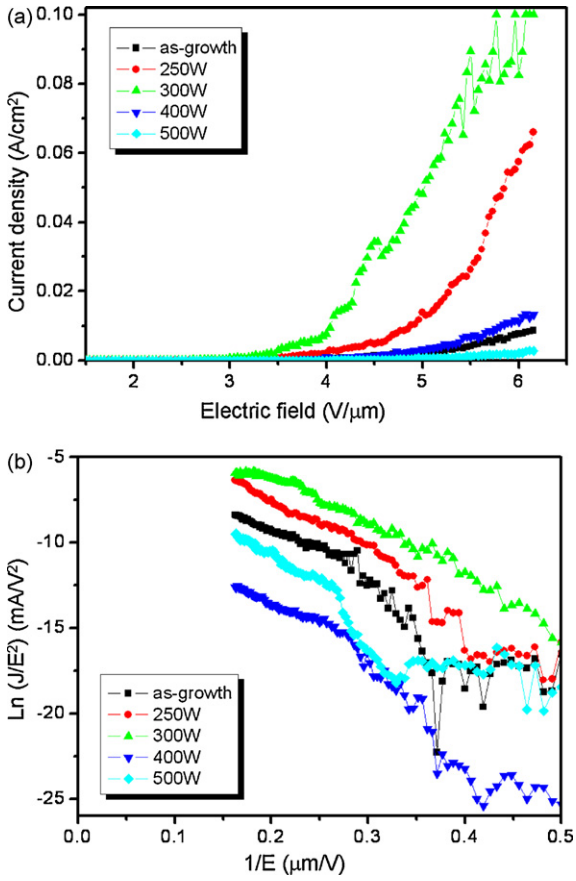


**Fig. 3.** (a) Emission current density vs. electric field curves of CNTs before and after Ar plasma treatment and (b) shows the Fowler–Nordheim plots correspondingly.

Thus, by taking logarithm on both sides of the equation, one obtains

$$\ln\left(\frac{J}{E^2}\right) = \ln\left(\frac{k_1 \beta^2}{\phi}\right) - k_2 \frac{\phi^{3/2}}{\beta}\left(\frac{1}{E}\right) \quad (3)$$

The field enhancement factor, $\beta$, can be calculated from the slope, $S$, of the FN plots [$\ln(J/E^2)$ vs. $1/E$] displayed in Fig. 3(b) according to the following relation:

$$S = -k_2 \frac{\phi^{3/2}}{\beta} \quad (4)$$

Using a work function $\phi$ = 4.95 eV for the multiwall CNTs [23], the values of the field enhancement factor, $\beta$, calculated for CNTs treated with various ICP powers of 250, 300, 400 and 500 W are 3008, 3463, 1956 and 1631, respectively (Table 1). The field enhancement factor is associated with geometrical shape of the emitter. Thus the maximum $\beta$ value obtained for the CNTs treated with 300 W Ar plasma indicates that, by properly manipulating the post-treatment conditions, there is a way of improving the emission characteristics of the CVD grown CNTs. In Fig. 4, the dependence of turn-on field (defined as the electric field for obtaining an emission current density of 10 μA/cm$^2$) and the threshold field on the CNTs for various conditions are presented. The turn-on field decreases from 3.6 to 2.2 V/μm with increasing Ar plasma post-treatment power. On the other hand, the threshold electric fields measured at an emission current density of 2 mA/cm$^2$ are 4.9 3.8, 3.4, 4.6 and 5.7 V/μm for the as-grown and Ar plasma post-treated CNTs with various powers ranged from 250 to

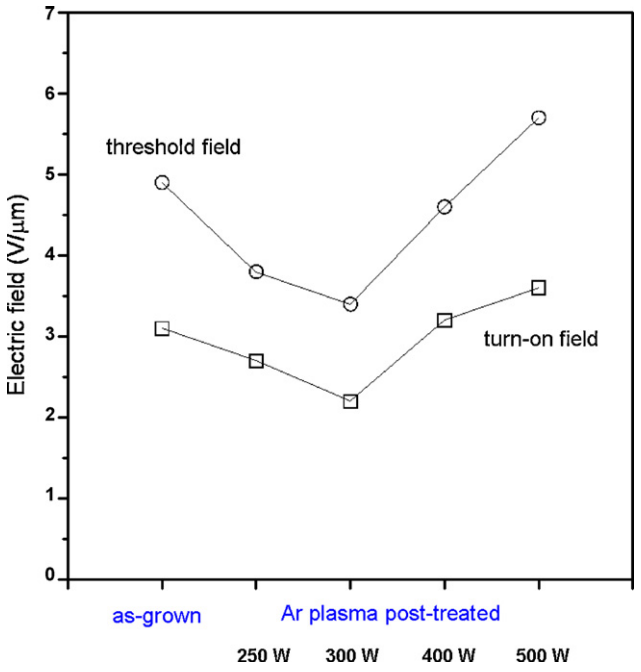


**Fig. 4.** The dependence of turn-on field (the electric field for emission current density of 10 μA/cm$^2$) and threshold field (the electric field for emission current density of 2 mA/cm$^2$) on the CNTs, before and after Ar plasma treatment with various powers.

500 W, respectively. We note that when the post-treatment power exceeds 400 W the emission properties of the CNTs degraded markedly, which might be a direct consequence of the serious damages induced to the CNTs seen in Fig. 2(f).

It is well known that one of the primary factors in determining the emission current is the field enhancement factor, more specifically the aspect ratio of CNTs [24]. The improvement on the field enhancement factor by proper Ar plasma treatment obtained in the present work appears to be also benefited from the increase of aspect ratio of Ar plasma post-treated CNTs (as clearly displayed in Fig. 2), which, in conjunction with the lower turn-on field due to generation of more emission-effective defective structures, are believed to be the primary reason giving rise to the near two orders magnitude enhancement in emission current. In addition, the energetic Ar plasma ions also contribute in removing the catalytic nanoparticles at the tip and change the CNTs morphology from blunt-like walls into the convex-shaped forms. These results indicate that proper practice of Ar plasma post-treatment can be an effective tool in optimizing the electron emission characteristics for CNTs.

## 4. Conclusions

In summary, the structural and field emission characteristics of MWCNTs synthesized by using thermal CVD method with high-density Ar plasma ICP-RIE post-treatment have been investigated systematically. Near two orders of magnitude improvement in emission current was obtained in CNTs treated with Ar plasma operated at a power of 300 W in an inductively coupled plasma chamber. The enhancements of field emission characteristics can be attributed to the combining effects of catalytic nanoparticles removal, the sharpening of CNT tip, as well as the development of bamboo-like tube structure. In addition to the structural modification of CNT walls, the ratio $I_D/I_G$ measured by Raman spectroscopy, which is an indication of amount of disorder-induced D-band signal over that from the stretching vibrating mode of crystalline graphite, shows that Ar plasma post-treatment also can helpful in removing the disordered tube segments. Finally, we note that the observations and the suggested prevailing mechanisms provided by Ar plasma post-treatment processes described here might be also applicable to other vertically aligned tube-like types of field emitters for improving their field emission characteristics. However, precautions must be taken to avoid extensive structural damage by overpowered energetic plasma ions.

## Acknowledgments

This work was partially supported by the National Science Council of Taiwan and I-Shou University, under Grant No.: NSC 97-2112-M-214-002-MY2, ISU97-07-01-04 and ISU97-S-02. JYJ is partially supported by the MOE-ATU program operated at NCTU.

## References

[1] S. Iijima, Nature 345 (1991) 56.
[2] R.H. Baughman, A.A. Zakhidov, W.A. de Heer, Science 297 (2002) 787.
[3] X.D. Li, H. Gao, W.A. Scrivens, D. Fei, X. Xu, M.A. Sutton, A.P. Reynolds, M.L. Myrick, Nanotechnology 15 (2004) 1416.
[4] J. Prabhuram, T.S. Zhao, Z.K. Tang, R. Chenm, Z.X. Liang, J. Phys. Chem. B 110 (2006) 5245.
[5] S.R. Jian, J.Y. Juang, Nanoscale Res. Lett. 3 (2008) 249.
[6] W.A. de Heer, W.S. Bacsa, A. Chatelain, T. Gerfin, R.H. Baker, L. Forro, D. Ugarte, Science 268 (1995) 845.
[7] W.A. de Heer, A. Chatelain, D. Ugarte, Science 270 (1995) 1179.
[8] S.S. Fan, M.G. Chaplind, N.R. Franklin, T.W. Tombler, A.M. Cassel, H.J. Dai, Science 283 (1999) 512.
[9] J.M. Bonard, N. Weiss, H. Kind, T. Stöckli, L. Forró, K. Kem, A. Châtelain, Adv. Mater. 13 (2001) 184.
[10] S.H. Jo, Y. Tu, Z.P. Huang, D.L. Carmhan, D.Z. Wang, Z.F. Ren, Appl. Phys. Lett. 82 (2003) 3520.
[11] A. Hart, B.S. Satyanarayana, W.I. Milne, J. Robertson, Appl. Phys. Lett. 74 (1999) 1594.
[12] Y.W. Zhu, F.C. Cheong, T. Yu, X.J. Xu, C.T. Lim, J.T.L. Thong, Z.X. Shen, C.K. Ong, Y.J. Liu, A.T.S. Wee, C.H. Sow, Carbon 43 (2005) 395.
[13] C.Y. Zhi, X.D. Bai, E.G. Wang, Appl. Phys. Lett. 81 (2002) 1690.
[14] R.T.K. Baker, Carbon 27 (1989) 315.
[15] S.K. Srivastava, V.D. Vankar, V. Kumar, V.N. Singh, Nanoscale Res. Lett. 3 (2008) 205.
[16] T. Ikuno, H. Furuta, T. Yamamoto, S. Takahashi, M. Kamizono, S. Honda, M. Katayama, T. Hirao, K. Oura, Surf. Interface Anal. 35 (2003) 15.
[17] S.R. Jian, Mater. Chem. Phys. 115 (2009) 740.
[18] L. Nilsson, O. Groening, C. Emmenegger, O. Kuettel, E. Schaller, L. Schlapbach, H. Kind, J.M. Bonard, K. Kem, Appl. Phys. Lett. 76 (2000) 2071.
[19] A.C. Ferrari, J. Robertson, Phys. Rev. B 61 (2000) 14095.
[20] S.H. Jo, D.Z. Wang, J.Y. Huang, W.Z. Li, K. Kempa, Z.F. Ren, Appl. Phys. Lett. 85 (2004) 810.
[21] R.H. Fowler, L.W. Nordheim, Proc. R. Soc. Lond. Ser. A 119 (1928) 173.
[22] L.W. Nordheim, Proc. R. Soc. Lond. Ser. A 121 (1928) 626.
[23] M. Shiraishi, M. Ata, Carbon 39 (2001) 1913.
[24] X.Q. Wang, M. Wang, P.M. He, Y.B. Xu, J. Appl. Phys. 96 (2004) 6752.